Sequential single-shot imaging of nanoscale dynamic interactions with a table-top soft x-ray laser

S. Carbajo,[1,2] I. D. Howlett,[1,2] F. Brizuela,[1,2] K. S. Buchanan,[3] M. C. Marconi,[1,2] W. Chao,[1,3] E. H. Anderson,[1,3] I. Artioukov,[5] A. Vinogradov,[5] J. J. Rocca,[1,2,3] and C. S. Menoni[1,2,*]

[1]National Science Foundation (NSF) Engineering Research Center for Extreme Ultraviolet Science and Technology, Colorado State University, Fort Collins, Colorado 80523, USA

[2]Department of Electrical and Computer Engineering, Colorado State University, Fort Collins, Colorado 80523, USA

[3]Department of Physics, Colorado State University, Fort Collins, Colorado 80523, USA

[4]Center for X-Ray Optics, Lawrence Berkeley Laboratory, Berkeley, California 94720, USA

[5]P. N. Lebedev Physical Institute, Moscow 119991, Russia

*Corresponding author: Carmen.Menoni@colostate.edu

Received March 19, 2012; revised May 28, 2012; accepted June 11, 2012; posted June 11, 2012 (Doc. ID 164934); published July 13, 2012

We demonstrate the first real-space recording of nanoscale dynamic interactions using single-shot soft x-ray (SXR) full-field laser microscopy. A sequence of real-space flash images acquired with a table-top SXR laser was used to capture the motion of a rapidly oscillating magnetic nanoprobe. Changes of 30 nm in the oscillation amplitude were detected when the nanoprobe was made to interact with stray fields from a magnetic sample. The table-top visualization of nanoscale dynamics in real space can significantly contribute to the understanding of nanoscale processes and can accelerate the development of new nanodevices.

OCIS codes: 110.0180, 180.7460, 340.7480.

Bright flashes of soft x-ray (SXR) light enable the imaging of nanostructures with a single shot [1–6]. Sequential single-shot flash SXR imaging makes it possible to freeze motion, opening the possibility to capture the dynamics of a variety of processes that include the motion of nanodevices and potentially that of nonrecurrent phenomena. This is in contrast to pump and probe time-resolved imaging used to study magnetodynamics with SXR synchrotron illumination, a stroboscopic measurement where typically several million events are averaged together before moving to the next time delay [7]. However, as of today, sequential single-shot SXR imaging has only been demonstrated in coherent diffractive and holographic experiments using free electron lasers [1,2]. These intensive post-image-processing techniques have femtosecond resolution and the potential for subnanometer spatial resolution. Alternatively, sequential single-shot images can be obtained by transmission electron microscopy, but space charge effects limit the attainable spatial and temporal resolution to tens of nanometers and tens of nanoseconds, respectively [8].

In this Letter, we demonstrate the first real-space recording of nanoscale dynamic interactions by single-shot SXR microscopy. A sequence of full-field flash images captured the dynamic interaction of a rapidly oscillating magnetic nanoprobe tip with the stray magnetic fields from a patterned magnetic sample. The nanoprobe tip motion was reconstructed from a sequence of SXR images acquired at selected times over the entire period of the tip oscillation. These results open new opportunities in material science and nanotechnology, such as the characterization of rapid motion in microelectromechanical/nanoelectromechanical devices, and the study of nanoscale processes in materials.

Sequential single-shot table-top SXR imaging was implemented using a compact microscope, schematically shown in Fig. 1 [3]. The nanoprobe tip was flash-illuminated with 10 μJ energy pulses ($2.4 \cdot 10^{12}$ photons/pulse) of 1.5 ns duration from a desk-top size 46.9 nm wavelength capillary discharge SXR laser with a spectral bandwidth of $\Delta\lambda/\lambda = 3.5\,10^{-5}$ [9,10]. The laser operates at repetition rates of up to 10 Hz [9]. The microscope uses a Sc/Si coated Schwarzschild condenser with 16% throughput at $\lambda =$ 46.9 nm [11]. The objective is a freestanding zone plate with 0.32 NA at $\lambda = 46.9$ nm and 10% efficiency in first order [12]. Images with ~1000× magnification were captured by a cooled back-illuminated array detector with 13.5 μm pixel size. The frequency of image acquisition was limited to a couple of images per minute by the readout time of the CCD. We have previously shown through static imaging of

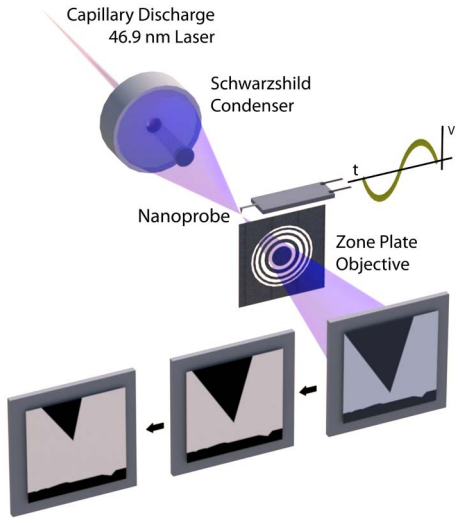

Fig. 1. (Color online) Schematic of the SXR laser-based sequential imaging setup used to record the oscillatory motion of a nanoprobe tip.

gratings that the combination of a 0.32 NA objective zone plate and a 46.9 nm laser yields images with a spatial resolution better than 54 nm [3]. Two different commercially available nanoprobe tips were used in the experiments, a high-aspect ratio Si tip and a Co-alloy coated standard magnetic tip that was magnetized along the tip axis prior to use.

The SXR images were acquired by triggering the laser at different times with respect to the tip driving signal. Each image was analyzed plotting the intensity profile along a vertical row of pixels containing the tip axis. The tip-to-surface separation was determined as the full width at half-maximum of the intensity profile. The accuracy of this measurement was ±12 nm. A set of over 100 sequential images were captured to map the entire period of the tip oscillation. Averaging of five independent sets of data allowed us to calculate the mean tip-to-surface distance with a precision of ±3 nm corresponding to 1 standard deviation. Figures 2(a) and 2(d) show four representative time-delayed single-shot images of the Si nanoprobe tip oscillating at the resonant frequency, 318.6 kHz, with ±250 nm amplitude. A comparison of the two top images shows the tip moved 57 nm in 0.41 μs. The position of the tip as a function of time for a complete oscillation is shown in Fig. 2(e). The flash images were subsequently integrated into an animation that illustrates the entire motion of the nanoprobe tip (see Media 1).

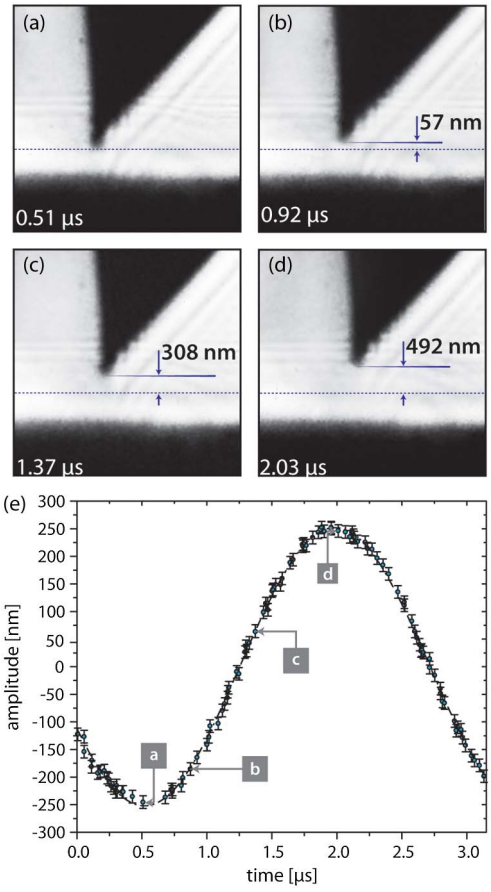

Fig. 2. (Color online) (a), (d) Time-delayed sequential SXR images illustrating the motion of a nanoprobe tip oscillating at a resonance frequency of 318.6 kHz with an oscillatory amplitude of ±250 nm. (e) Sequence of 100 single-shot images reproducing the motion of the tip over a full period.

The immunity of photon beams to electric and magnetic fields allows SXR light to probe the interaction of nanoscale objects in the presence of external fields, in contrast to electron probes. We recorded nanometer-scale variations in the motion of the magnetized Co-alloy coated nanoprobe tip induced by the interaction with stray magnetic fields created by a magnetic sample in a fashion that resembles the operation of standard magnetic force microscopes. The low magnetic moment Co-alloy tip with a nominal spring constant of 0.7 N/m oscillating at a resonant frequency of 65.6 kHz was placed above a magnetic sample consisting of a 1∶1 array of 2 μm wide strips patterned on a 40 nm thick Permalloy film deposited onto a Si wafer. The Permalloy microstrips exhibit strong uniaxial shape anisotropy and hence remain magnetized along the axis at remanence. The magnetic nanoprobe tip was positioned close to the end of the microstrips where the stray magnetic field is highest, and in between where the stray field is nearly zero. At the minimum in the oscillation the tip was separated by ~150 nm from the microstrips. As the resonating magnetic nanoprobe tip approached, a Permalloy microstrip, the stray magnetic fields exerted a magnetic force with a gradient of the order of 10^{-2} N/m, which deflected the tip either toward or away from the sample surface depending on the sign of the magnetization. The plot of Fig. 3(a) shows the measured tip loci versus time when positioned immediately above a magnetic microstrip where the magnetic strength is largest. An increase in the amplitude of the oscillation of (30 ± 3) nm with respect to the natural

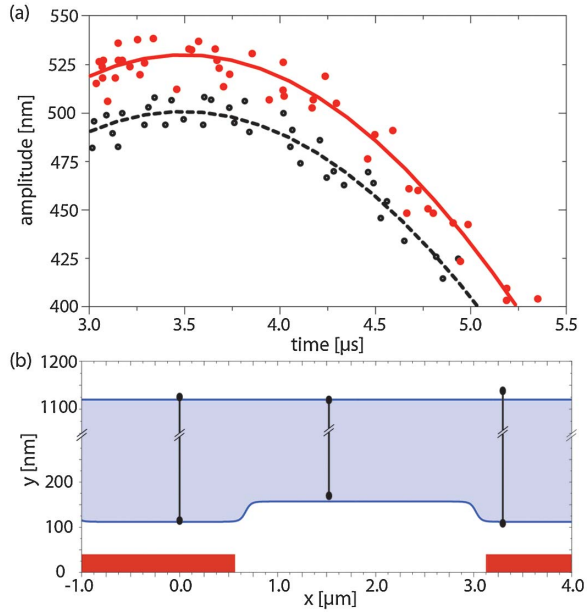

Fig. 3. (Color online) (a) Measured increase of the magnetic tip oscillation amplitude when the tip is located above a magnetized microstrip (red trace) as compared to that observed when the tip is placed in the region between strips, where the field is negligible and the tip follows its natural oscillation (black trace). (b) Computed amplitude of the tip oscillation (blue shaded region) relative to its position in respect to the Permalloy microstrips (in red). The dots (black) represent the measured maximum and minimum of the tip oscillation.

oscillation amplitude was measured. The extrema of the tip oscillation relative to the magnetic surface determined from the images are represented in Fig. 3(b) by the black dots.

The variations in the oscillation amplitude due to the interaction with the stray magnetic fields were computed using a model that considers the magnetic tip to be a perturbed harmonic oscillator in the presence of actuating forces that arise from a magnetic dipole–dipole interaction. The stray fields of the Permalloy microstrip at the tip location were calculated using the Object Oriented MicroMagnetic Framework (OOMMF) [13]. The stray fields were highly nonuniform, showing large magnetic strength on the edges of the Permalloy strip. The force gradients were calculated using established values of magnetization of $8\,10^5$ A/m and $14\,10^5$ A/m for Permalloy and Co-alloy, which, for the volumes under consideration, result in magnetic moments of $4.1\,10^{-17}$ A m^2 and $6.4\,10^{-13}$ A m^2 for the tip and microstrips, respectively. The nonuniform stray force fields effectively change the restoring force in the oscillating magnetic tip through a term that is proportional to the magnetic force gradient. As a consequence, when driving the tip at a fixed frequency, the amplitude and phase of the tip oscillation are modified. The computed loci of the tip during a full period oscillation, represented by the blue region in Fig. 3(b), are in good agreement with the experimental results.

In summary, we have directly visualized nanoscale dynamic phenomena using bright flashes from a compact SXR laser. The ability to visualize nanoscale motion on a table-top will impact the development of nanoelectromechanical devices. Moreover, the use of a similar SXR microscope in a reflection configuration [14] will allow one to visualize nanoscale material surface dynamics, including nanoscale laser ablation and nanomachining, and studies of material dislocation dynamics, nucleation, and growth. Furthermore, this table-top SXR laser dynamic imaging approach is readily scalable in wavelength and temporal resolution. The recent advances in saturated table-top SXR laser sources, that now provide picosecond pulses with energies >10 μJ per pulse at 13.9 nm [15], will open the possibility to visualize ultrafast dynamics with a few tens of nanometers spatial resolution and picosecond time resolution. Further advances in injection-seeding table-top SXR lasers that are expected to produce high-energy femtosecond pulses will make it possible to extend this technique to the femtosecond range [16].

This work was supported by the National Science Foundation (NSF) Engineering Research Center (ERC) for Extreme Ultraviolet Science and Technology under NSF Award EEC-0310717 using equipment developed under NSF Award MRI-ARRA 09-561, and by the Chemical Sciences, Geosciences and Biosciences Division, Office of Basic Energy Sciences, U.S. Department of Energy. K. S. Buchanan was also supported by NSF award number 0907706. We acknowledge the contributions of D. T. Attwood, Y. Liu, A. Sakdinawat, A. G. Ponomareko, V. V. Kondratenko, Y. Sun, and M. Wu. S. Carbajo acknowledges support of the Basque Government PFPPI.

References

1. H. N. Chapman, S. P. Hau-Riege, M. J. Bogan, S. Bajt, A. Barty, S. Boutet, S. Marchesini, M. Frank, B. W. Woods, W. H. Benner, R. A. London, U. Rohner, A. Szoke, E. Spiller, T. Moller, C. Bostedt, D. A. Shapiro, M. Kuhlmann, R. Treusch, E. Plonjes, F. Burmeister, M. Bergh, C. Caleman, G. Huldt, M. M. Seibert, and J. Hajdu, Nature **448**, 676 (2007).
2. A. Barty, S. Boutet, M. J. Bogan, S. Hau-Riege, S. Marchesini, K. Sokolowski-Tinten, N. Stojanovic, R. A. Tobey, H. Ehrke, A. Cavalleri, S. Dusterer, M. Frank, S. Bajt, B. W. Woods, M. M. Seibert, J. Hajdu, R. Treusch, and H. N. Chapman, Nat. Photon. **2**, 415 (2008).
3. C. A. Brewer, F. Brizuela, P. Wachulak, D. H. Martz, W. Chao, E. H. Anderson, D. T. Attwood, A. V. Vinogradov, I. A. Artyukov, A. G. Ponomareko, V. V. Kondratenko, M. C. Marconi, J. J. Rocca, and C. S. Menoni, Opt. Lett. **33**, 518 (2008).
4. M.-C. Chou, R.-P. Huang, P.-H. Lin, C.-T. Huang, S.-Y. Chen, H.-H. Chu, J. Wang, and J.-Y. Lin, Opt. Lett. **34**, 623 (2009).
5. H. T. Kim, I. J. Kim, C. M. Kim, T. M. Jeong, T. J. Yu, S. K. Lee, J. H. Sung, J. W. Yoon, H. Yun, S. C. Jeon, I. W. Choi, and J. Lee, Appl. Phys. Lett. **98**, 1105 (2011).
6. A. Ravasio, D. Gauthier, F. R. N. C. Maia, M. Billon, J. P. Caumes, D. Garzella, M. Geleoc, O. Gobert, J. F. Hergott, A. M. Pena, H. Perez, B. Carre, E. Bourhis, J. Gierak, A. Madouri, D. Mailly, B. Schiedt, M. Fajardo, J. Gautier, P. Zeitoun, P. H. Bucksbaum, J. Hajdu, and H. Merdji, Phys. Rev. Lett. **103**, 028104 (2009).
7. H. Stoll, A. Puzic, B. van Waeyenberge, P. Fischer, J. Raabe, M. Buess, T. Haug, R. Hollinger, C. Back, D. Weiss, and G. Denbeaux, Appl. Phys. Lett. **84**, 3328 (2004).
8. J. S. Kim, T. LaGrange, B. W. Reed, M. L. Taheri, M. R. Armstrong, W. E. King, N. D. Browning, and G. H. Campbell, Science **321**, 1472 (2008).
9. S. Heinbuch, M. Grisham, D. Martz, and J. J. Rocca, Opt. Express **13**, 4050 (2005).
10. J. J. Rocca, V. N. Shlyaptsev, F. G. Tomasel, O. D. Cortazar, D. Hartshorn, and J. L. A. Chilla, Phys. Rev. Lett. **73**, 2192 (1994).
11. I. A. Artioukov, A. V. Vinogradov, V. E. Asadchikov, Y. S. Kasyanov, R. V. Serov, A. I. Fedorenko, V. V. Kondratenko, and S. A. Yulin, Opt. Lett. **20**, 2451 (1995).
12. E. H. Anderson, IEEE J. Quantum Electron. **42**, 27 (2006).
13. M. J. Donahue and D. G. Porter, "OOMMF user's guide, version 1.0" (National Institute of Standards and Technology, 1999), p. 6376.
14. F. Brizuela, G. Vaschenko, C. Brewer, M. Grisham, C. Menoni, M. Marconi, J. Rocca, W. Chao, J. Liddle, E. Anderson, D. Attwood, A. Vinogradov, I. Artioukov, Y. Pershyn, and V. Kondratenko, Opt. Express **13**, 3983 (2005).
15. D. H. Martz, D. Alessi, B. M. Luther, Y. Wang, D. Kemp, M. Berrill, and J. J. Rocca, Opt. Lett. **35**, 1632 (2010).
16. Y. Wang, E. Granados, F. Pedaci, D. Alessi, B. Luther, M. Berrill, and J. J. Rocca, Nat. Photon. **2**, 94 (2008).